

2009

Parameter Optimization for Image Denoising Based on Block Matching and 3D Collaborative Filtering

Ramu Pedada
Old Dominion University

Emin Kugu
Old Dominion University

Jiang Li
Old Dominion University, jli@odu.edu

Zhanfeng Yue
Precision Imaging Systems

Yuzhong Shen
Old Dominion University, yshen@odu.edu

See next page for additional authors

Follow this and additional works at: https://digitalcommons.odu.edu/ece_fac_pubs



Part of the [Bioimaging and Biomedical Optics Commons](#), [Biomedical Commons](#), [Equipment and Supplies Commons](#), and the [Theory and Algorithms Commons](#)

Original Publication Citation

Pedada, R., Kugu, E., Li, J., Yue, Z., & Shen, Y. (2009). Parameter optimization for image denoising based on block matching and 3D collaborative filtering. In J.P.W. Pluim & B.M. Dawant (Eds.), *Medical Imaging 2009: Image Processing, Proceedings of SPIE Vol. 7259 (725925)*. SPIE of Bellingham, WA.
<https://doi.org/10.1117/12.812202>

This Conference Paper is brought to you for free and open access by the Electrical & Computer Engineering at ODU Digital Commons. It has been accepted for inclusion in Electrical & Computer Engineering Faculty Publications by an authorized administrator of ODU Digital Commons. For more information, please contact digitalcommons@odu.edu.

Authors

Ramu Pedada, Emin Kugu, Jiang Li, Zhanfeng Yue, Yuzhong Shen, Josien P.W. Pluim (Ed.), and Benoit M. Dawant (Ed.)

Parameter Optimization for Image Denoising Based on Block Matching and 3D Collaborative Filtering

Ramu Pedada^a, Emin Kugu^a, Jiang Li^a, Zhanfeng Yue^b, Yuzhong Shen^a

^aDept. of Electrical and Computer Engineering, Old Dominion University, Norfolk VA

^bPrecision Imaging Systems, Cary, NC 27519

ABSTRACT

Clinical MRI images are generally corrupted by random noise during acquisition with blurred subtle structure features. Many denoising methods have been proposed to remove noise from corrupted images at the expense of distorted structure features. Therefore, there is always compromise between removing noise and preserving structure information for denoising methods. For a specific denoising method, it is crucial to tune it so that the best tradeoff can be obtained. In this paper, we define several cost functions to assess the quality of noise removal and that of structure information preserved in the denoised image. Strength Pareto Evolutionary Algorithm 2 (SPEA2) is utilized to simultaneously optimize the cost functions by modifying parameters associated with the denoising methods. The effectiveness of the algorithm is demonstrated by applying the proposed optimization procedure to enhance the image denoising results using block matching and 3D collaborative filtering. Experimental results show that the proposed optimization algorithm can significantly improve the performance of image denoising methods in terms of noise removal and structure information preservation.

Keywords: Block matching, collaborative filtering, cost functions, multiobjective optimization, Pareto front

1. INTRODUCTION

Magnetic resonance imaging (MRI) is a medical imaging technique primarily used in radiology to visualize the structure of a body. In clinical practice, MRI is used to distinguish pathologic tissue from normal tissue. Clinical MRI images are generally corrupted by random noise during acquisition with blurred subtle structure features.^[1] Many denoising methods have been proposed to remove noise from corrupted images at the expense of distorted structure features.^[2] Therefore, there is always a trade-off between noise removal and structure information preservation for denoising methods. In order to effectively remove noise and to preserve structure information, it is crucial to tune denoising methods so that the best balance between the two conflicting objectives can be obtained. In this paper, we propose an optimization procedure that can automatically tune parameters involved in denoising algorithms. The procedure will produce a set of optimal parameters that enable the designer to make the best trade-offs between noise removal and structure information preservation. We applied the proposed algorithm on a block matching and 3D collaborative filtering algorithm for MRI image denoising.^[3]

Image denoising using block matching and 3D collaborative filtering is a recently developed denoising algorithm based on an enhanced sparse representation in the transform domain. Block matching is used to stack 2D blocks of a given image that are similar to a reference block. The matched blocks are stacked together to form a 3D array. Collaborative filtering is a special procedure used to deal with these 3D groups. The major steps involved in collaborative filtering are applying a 3D transform to the formed groups followed by shrinkage of transform coefficients and inverse wiener filtering. The reason for using 3D filtering is that 2D transforms cannot achieve good sparsity for all kinds of images. Using 3D arrays instead of 2D blocks enhances the sparsity so that the noise can be well attenuated by shrinkage of transform coefficients. The main disadvantage of this denoising algorithm is that a lot of interesting structure information is lost during the process of denoising. Structure information should be preserved for effective image analysis. In this paper, we define several cost functions to assess the quality of noise removal and that of structure information preserved

*Send correspondence to Jiang Li: JLi@odu.edu Tel: 1-757-6836748.

in the denoised image. Strength Pareto Evolutionary Algorithm (SPEA2) is used to simultaneously optimize the cost functions by modifying parameters associated with the denoising method. Experimental results show that the proposed optimization algorithm can significantly improve the performance of image denoising methods in terms of noise removal and structure information preservation.

2. AN EXISTING DENOISING ALGORITHM

Before presenting the proposed optimization procedure, a brief review of a recently developed image denoising method^[3,13] based on block matching and 3D collaborative filtering, is discussed in this section.

2.1 Algorithm Background

Many transformation based denoising methods rely on some explicit or implicit assumptions about the true image in order to separate it properly from the random noise. These methods assume that the true signal can be well approximated by a linear combination of basis functions. That is, the signal is sparsely represented in the transform domain, but the shrinkage of transform domain coefficients is ineffective with sparse representation of an image. For example, 2D DCT cannot sparsely represent sharp transitions such as edges in an image. Generally, a 2D transform cannot achieve good sparsity because of the great variety of natural images. 2D orthogonal transforms can achieve sparse representation only for some particular image patterns. To achieve a good sparsity for any natural image, 3D data arrays can be used instead of 2D fragments. In this novel image denoising strategy, the enhanced sparse representation in the transform domain is achieved by grouping similar 2D fragments of the image into 3D arrays called "groups". Collaborative filtering is a special procedure developed to deal with these 3D groups. 3D transformations are applied to the 3D groups followed by shrinkage of transform coefficients, and the inverse 3D transform subsequently. Due to the similarity between the grouped blocks, the 3D transform can achieve a highly sparse representation of the true signal so that the noise can be well separated by shrinkage.

2.2 Grouping and Collaborative Filtering

Grouping is the concept of collecting similar d -dimensional fragments of a given signal to form a $d+1$ dimensional data structure. For an image, a 3D array is formed by stacking together similar 2D image fragments. A simpler and effective grouping strategy for images is matching - a method for finding fragments similar to a given reference.^[4] This can be accomplished by pair-wise testing of similarities between the reference fragment and the other fragments located at other locations. A fragment is said to be matched with the reference fragment if the distance between these two is smaller than a specified threshold. The fragments satisfying this condition are considered as members of the group, and the reference fragment is considered as "centroid" for the group. The block-matching approach is used extensively for motion estimation in video compression techniques. An illustrative example of grouping by block-matching of two images is given in Fig. 1, where a reference block is denoted by "R" and the ones matched to it are denoted in rectangular boxes.

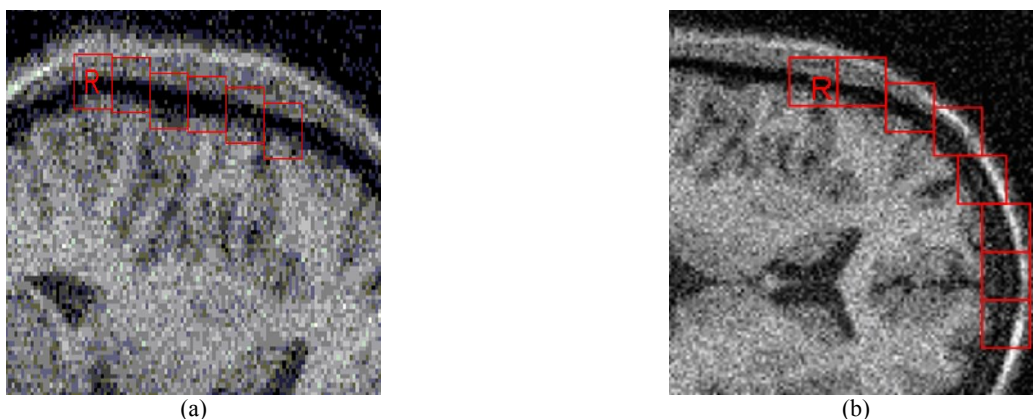


Fig. 1: Block Matching

After grouping the 2D image fragments to form a 3D array, collaborative filtering is applied to 3D arrays. Given a group of n estimates, the collaborative filtering of the group produces n estimates, one for each of the grouped fragments. Effective collaborative filtering can be realized as shrinkage in the transform domain. Given $d + 1$ dimensional groups of similar fragments, the first step in collaborative shrinkage is to apply a $(d + 1)$ -dimensional linear transform to the group.

Then soft and hard-thresholding or Wiener filtering is used to shrink the transform coefficients to attenuate the noise. The final step in collaborative filtering is to apply an inverse transform to produce estimates of all grouped fragments. Generally, groups formed from natural images as shown in Fig. 1 are characterized by intra-fragment correlation (appears between pixels of each grouped fragment) and inter-fragment correlation (appears between the corresponding pixels of different fragments). The 3D transform can take advantage of both correlations and produce a sparse representation of the true signal in the group, which makes the shrinkage very effective when attenuating the noise.

2.3 Outline of the Denoising Algorithm

In the denoising algorithm, grouping is realized by block matching, and collaborative filtering is accomplished by shrinkage in a 3D transform domain. All the image fragments used in matching are square blocks of fixed size. The outline of the algorithm is described as follows:

Step 1. Basic Estimate.

a) *Block-Wise Estimate.* For each block in the noisy image

i) *Grouping.* Apply the block matching technique to find similar blocks and stack them to form a 3D array.

ii) *Collaborative hard-thresholding.* Apply a 3D transform to the formed groups and apply hard thresholding to attenuate the noise and invert the 3D transform to produce estimates of all grouped blocks to their original positions.

b) *Aggregation.* Compute the weighted average of all the overlapping block-wise estimation results in the basic estimate.

Step 2. Final Estimate.

After obtaining the basic estimate from step 1, perform the following steps.

a) *Block-wise estimates.* For each block,

i) *Grouping.* Apply block matching for the basic estimate to find similar blocks and form two groups, one from the noisy image and one from the basic estimate.

ii) *Collaborative Wiener filtering.* Apply a 3D transform on both groups. Perform Wiener filtering on the noisy one to produce estimates of all grouped blocks by applying the inverse 3D transform on the filtered coefficients, and return the estimates of the blocks to their original positions.

b) *Aggregation.* The final estimate of the true image is computed by aggregating all of the local estimates obtained by using the weighted average. The reason for the second step in the above procedure is that, instead of a noisy image, using the basic estimate improves the grouping. The flow chart of the algorithm is illustrated in Fig. 2. In the figure, operations surrounded by dashed lines are repeated for each processed block marked with "R" [13].

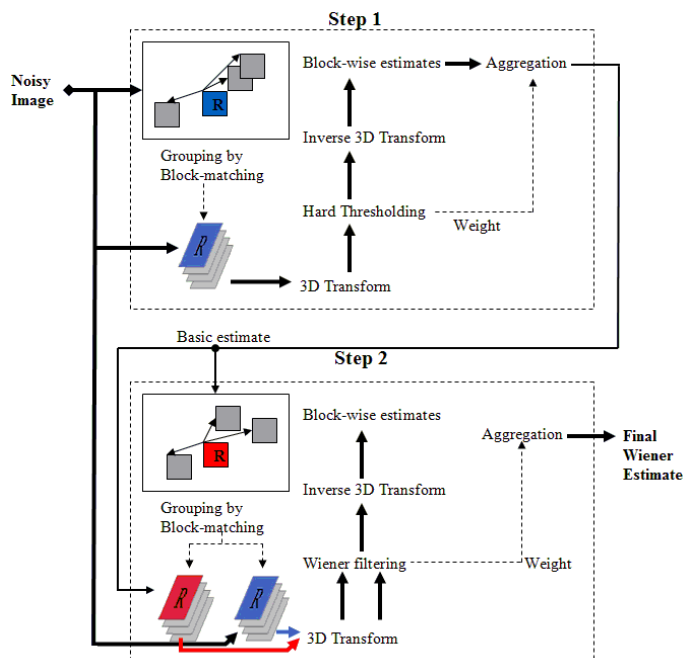


Fig. 2: Flow chart of the algorithm

2.4 Algorithm Implementation

There are a set of parameters associated with the described algorithm as follows,

1. N_2 : Maximum number of similar blocks (maximum size of the 3rd dimension of a 3D array).
2. N_s : Size of the search neighborhood for full-search block-matching (BM). It must be odd.
3. τ_{match} : Threshold for the block distance (d-distance)
4. λ_{thr2D} : Threshold parameter for the coarse initial denoising used in the d-distance (distance between the reference block and the matched block) measure.
5. λ_{thr3D} : Threshold parameter for the hard-thresholding in 3D transform domain.
6. β : Parameter of the 2D Kaiser window used in reconstruction. Kaiser window is used to reduce the border effects that can appear due to the usage of certain 2D transforms.
7. N_2_{Wiener} : Maximum number of similar blocks for step 2.
8. N_s_{Wiener} : Length of side of search neighborhood in step 2.
9. $\tau_{\text{match}_{\text{Wiener}}}$: Threshold for block distance in step 2.
10. β_{Wiener} : 2D Kaiser window used in step 2.
11. σ : Standard deviation of noise.
12. N_1 : $N_1 \times N_1$ is the block size used for the hard-thresholding (HT) filtering.
 1. This is the block size of the Kaiser window used during the shrinkage of transform coefficients using hard-thresholding.
13. N_{step} : Sliding step to process every next reference block. Rather than sliding by one pixel to every next reference block, use a step of N_{step} pixels to move to the next reference block.
14. N_1_{Wiener} : $N_1 \times N_1$ is the block size used for the HT filtering in step 2.
15. $N_{\text{step}_{\text{Wiener}}}$: Sliding step to process every next reference block in step 2.

The values of above parameters may vary between certain thresholds. For a given noisy image, a different set of parameters will result in a different denoised image. Based on several experiments, the authors have proposed a set of parameters that produce best results, used them as default parameters. Fig. 3(a) shows a noise free MR image obtained from brain web^[5]. Additive white Gaussian noise with zero mean and standard deviation of 25% is added to the noise free image shown in Fig. 3(b). The result of the denoising algorithm with default parameter values is shown in Fig. 3(c).

After applying the denoising algorithm to the noisy image shown in Fig. 3(b), many interesting features in the image are lost in the process of denoising. In Fig. 3(c), it is clear that many edges in the images are lost due to extra smoothing. For effective image analysis, edge information of an image should be preserved along with a good quality of denoising. The main drawback of the current denoising algorithm is that the interesting structures in the image are not preserved well. This problem exists not only with the current denoising algorithm but also with many other denoising algorithms. Optimal results can be obtained through parameter selection, which is described in the following section.

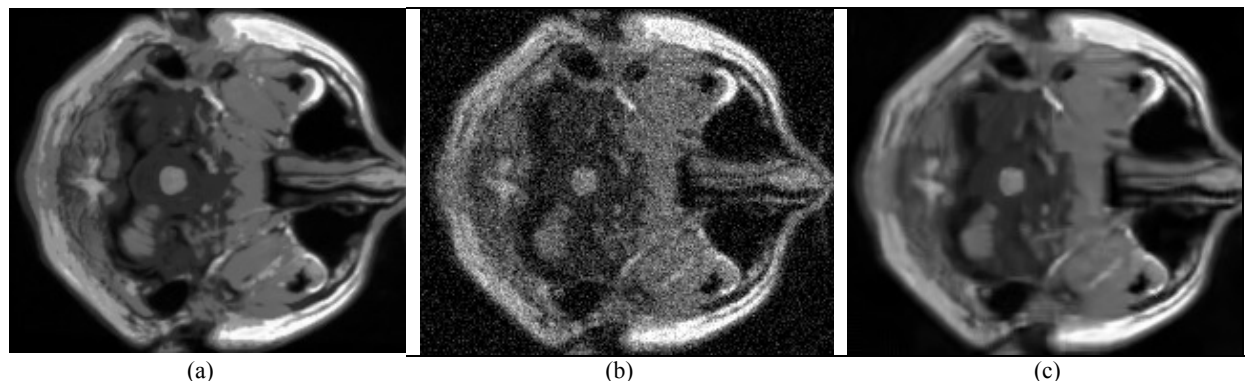


Fig. 3: (a) Noise free image, (b) Noise added image $\sigma = 25$, (c) Denoised image

3. THE PROPOSED PARAMETER OPTIMIZATION METHOD

The most common problem with existing denoising methods is that some interesting structures in the image will be removed from the image during the denoising process. Such interesting structures in an image often correspond to

discontinuities in the image that provide important information. In MRI image analysis, discontinuities are very important as they are used to differentiate the pathological tissue from the normal tissue. Optimizing the outcome of the denoising method is crucial for effective image analysis. In the proposed research, multiobjective evolutionary techniques are used for the optimization procedure.

3.1 Multiobjective Optimization

Many real world applications have several conflicting objectives. The objective functions are difficult to be expressed in a closed form. A practical solution is to look at this parameter setting problem as a multiobjective evolutionary problem.^[6] Multiobjective optimization problems occur whenever optimal decisions need to be taken in the presence of trade-offs between conflicting objectives. Maximizing profit and minimizing the cost of a product, maximizing performance and minimizing fuel consumption of a vehicle are examples of multi-objective optimization problems. It is rare that there is a single solution that simultaneously optimizes all the objectives. Therefore, when dealing with multiobjective optimization problems, we normally look for a set of optimal solutions, and a designer can make trade-offs within this set. The resulting solution set is said to be Pareto optimal and the solutions are said to be Pareto efficient^[7]. The plot of the Pareto optimal solutions in the objective space is called the Pareto front. In this paper, we applied the SPEA2 algorithm^[8] to obtain the Pareto optimal solutions for the denoising algorithm.

3.2 Cost Functions

We define two costing functions to assess the quality of noise removal and structure information preservation in this section.

3.2.1 Mean Square Error (MSE)

Mean square error (MSE) is one means to quantify the amount by which the denoised image differs from the original noise free image, and is used to quantify the quality of noise removal. For a denoising method, a low value of MSE is preferable since the denoised image will be as close as possible to the noise free image. In the current context, MSE is calculated between the denoised image and the ground truth (noise free) image. Let $f(x,y)$ be the noise free image of size

$M \times N$ and $\hat{f}(x, y)$ the output of the denoising algorithm, MSE is calculated as follows:

$$MSE = \frac{1}{MN} \sum_{i=1}^M \sum_{j=1}^N (f(i, j) - \hat{f}(i, j))^2 \quad (1)$$

3.2.2 Entropy

Entropy is a statistical measure of randomness or information contained in an image. Let $D(x, y)$ be the difference between $f(x, y)$ and $\hat{f}(x, y)$ for the case of white Gaussian noise, if the power spectrum of $D(x, y)$ is white, the denoising is uniform for all frequency components and structure information in the original image is preserved. On the other hand, if the power spectrum is concentrated only in particular frequencies, this indicates that the features in the original image corresponding to those frequency components are lost during the denoising process. Therefore, we compute the entropy for the difference image's power spectrum as a quality measure of structure information preservation and lower entropy value is preferred. Assume the information content in an image can be represented with N gray level values and x occurs with a probability of $p(x)$, then the entropy is given as

$$Entropy = - \sum_{i=1}^N p(x_i) \log(p(x_i)) \quad (2)$$

Entropy is typically measured in bits per symbol (gray level).

3.2.3 Second Derivative

The second derivative of the output image $\hat{f}(x, y)$ contains edge information in the image. In some clinical practices, the edge information in images is desired to be preserved or enhanced. Standard deviation (SD) of second derivative of the denoised image gives clues on how much information is kept in the images. We use the SD of the second derivative of the denoised image to measure the structure information in the image. Since the edges are to be preserved, a higher

value of SD is preferred. Therefore, $1/SD$ should be minimized. The second derivative of an image can be approximated by convoluting the image with a Laplacian mask,

$$\begin{pmatrix} -1 & -1 & -1 \\ -1 & 8 & -1 \\ -1 & -1 & -1 \end{pmatrix} \quad (3)$$

3.3 Problem Formulation

We consider minimizing two cost functions at one time in this paper. Let $f_1(\vec{x})$ and $f_2(\vec{x})$ denote the defined cost functions, where \vec{x} is an n -dimensional threshold vector. The values of cost functions are obtained by modifying the parameters associated with the denoising algorithm. The value of n depends on the denoising algorithm being used. In order to minimize the two conflicting functions, we formulate it as a multiobjective optimization problem^[9],

$$\min \vec{f}(\vec{x}) = \{f_1(\vec{x}), f_2(\vec{x})\} \quad (4)$$

Subject to

$$\left\{ \begin{array}{l} x_1 \in (0, 36], \\ x_2 \in (0, 89], \\ x_3 \in (0, 10000], \\ x_4 \in (0, 1], \\ x_5 \in (0, 5], \\ x_6 \in (0, 4], \\ x_7 \in (0, 36], \\ x_8 \in (0, 89], \\ x_9 \in (0, 10000], \\ x_{10} \in (0, 5], \\ x_{11} \in (1, 15], \\ x_{12} \in (2, 32], \\ x_{13} \in (4, 32], \\ x_{14} \in (2, 32], \\ x_{15} \in (4, 36]. \end{array} \right.$$

where x_1 to x_{15} correspond to parameters 1 to 15 defined in Section 2.4 respectively,

$$\vec{x} = \{x_1, \dots, x_{15} \mid x_1, \dots, x_{11} \in \mathbf{R}, x_{12}, \dots, x_{15} \in I\} \quad (5)$$

The range of parameter values are chosen such that the final optimal set contains all solutions of interest. The global optima of the multiobjective optimization problem is the Pareto front determined by evaluating each member of the Pareto optimal set.^[10] The Pareto optimal set consists of solutions that are not dominated by any other solution. A solution, \vec{x}_1 , is said to dominate, (\succ), \vec{x}_2 , if the objective vector, $f_1(\vec{x}_1)$ is less than or equal to $f_2(\vec{x}_2)$ in all attributes and strictly less than at least one attribute,

$$\left\{ \begin{array}{l} \vec{x}_1 \succ \vec{x}_2, \text{ iff} \\ \forall i \in \{1, 2\} : f_i(\vec{x}_1) \leq f_i(\vec{x}_2) \wedge \exists j \in \{1, 2\} : f_j(\vec{x}_1) < f_j(\vec{x}_2). \end{array} \right. \quad (6)$$

The plot of the objective functions whose vectors are in the Pareto optimal set is called Pareto front. The decision maker can select the solution satisfying all the objectives from the Pareto optimal set.^[11]

3.4 SPEA2 Algorithm

SPEA2^[12] is a technique to find or approximate the Pareto optimal set for multiobjective optimization problems. In this section, we briefly describe the SPEA2 algorithm, which has four steps:

1. Randomly initialize the solution population.
2. Evaluate and assign a fitness value for each individual in the population according to its performance.
3. Select individuals based on their performance so that better individuals are more likely to be selected for producing the next generation.
4. Use crossover and mutation to produce the next generation from the selected individuals.

In the current optimization procedure, lower fitness values of cost functions indicate better performance. Steps 2 through 4 are repeated until the generation number is reached. SPEA2 differs from a standard genetic algorithm in the following aspects.

Environmental Selection: Apart from regular population, which is used in the genetic algorithm, in SPEA2 an archive that contains all the nondominated solutions from the previous generation is maintained. A member of the archive is removed if the following conditions are satisfied.

1. A dominant solution is found in the current generation or
2. The archive maximum size is reached and the member's performance is worse than that of others.

Fitness Evaluation: Let P_t and \bar{P}_t denote the population and archive respectively; each individual i in P_t and \bar{P}_t is assigned a strength value $S(i)$ that denotes the number of dominant solutions,

$$S(i) = \left\| \left\{ j \mid j \in P_t + \bar{P}_t \wedge i \succ j \right\} \right\|, \quad (7)$$

where $\|\cdot\|$ represents the cardinality of a set, $+$ represents the multiset union and \succ represents the Pareto dominance relation. The raw fitness value $R(i)$ is given as

$$R(i) = \sum_{j \in P_t + \bar{P}_t, j \succ i} S(j) \quad (8)$$

The final fitness values for the i th individual is given as

$$F(i) = R(i) + D(i), \quad (9)$$

where $D(i)$ are the density values estimated as

$$D(i) = \frac{1}{\delta_i^k + 2}, \quad (10)$$

and δ_i^k denotes the k th nearest distance for the i th individual among P_t and \bar{P}_t in objective space. k is usually set as $\sqrt{N + \bar{N}}$, where N represents the population size and \bar{N} represents the archive size.

Mating Selection: In SPEA2, all candidates are chosen from the archive using a binary tournament selection procedure. In the binary tournament selection, we randomly select two individuals and only the better one survives.

3.5 Algorithm Outline

Step 1. Initialization:

Initialize the population size, (N), archive size, (\bar{N}), and generation number, (T). The typical values are $N = 100$, $\bar{N} = 100$, and $T = 200$. Randomly generate solution set P_t , set \bar{P}_t empty. Set $t = 0$.

Step 2. Termination:

Nondominated parameters in \bar{P}_t are returned as the final result if $t > T$.

Step 3. Fitness Evaluation:

Evaluate each solution in P_t and \bar{P}_t by running the denoising algorithm on a given image. The fitness value for each solution is then calculated as above.

Step 4. Environmental Selection:

Copy all the individuals in P_t and \bar{P}_t to \bar{P}_{t+1} . Delete the worst solutions in \bar{P}_{t+1} if the size of \bar{P}_{t+1} exceeds N . If the size is less than N , copy the dominant solutions in P_t that have smaller fitness values.

Step 5. Mating Selection:

Using the binary tournament procedure, select 100 individuals from \bar{P}_t with replacement.

Step 6. Reproduce:

The next generation is reproduced using mutation and standard crossover procedures. The probability values of crossover and mutation are chosen as 0.9 and 0.001 respectively. Store the results in \bar{P}_{t+1} and increment t by 1 and go to step 2.

4. EXPERIMENT AND RESULTS

We ran the proposed optimization procedure several times using images from the brainweb database⁵. We minimized two cost functions at one time, and produced a Pareto front for each run. We chose several points on the Pareto front, where each point on the curve corresponds to one parameter set of the denoising algorithm, and ran the denoising algorithm using the parameters. The results from different parameters, including that from the default parameter set, were compared.

4.1 Simulated Brain Database

All the images used for the testing optimization procedure are obtained from the brain-web, which contains a simulated brain database (SBD)^[5]. SBD contains simulated brain MRI data based on two anatomical models: normal and multiple sclerosis (MS). This contains full 3-dimensional data volumes simulated using three sequences (T1-, T2-, and proton-density- (PD-) weighted MRI images) and a variety of slice thicknesses, noise levels, and levels of intensity non-uniformity. These data are available for viewing in three orthogonal views (transversal, sagittal, and coronal), and for downloading free of charge.

4.2 Results from Default Parameters

Before presenting the optimized results, the results of the denoising algorithm using default parameters are presented in this section. Fig. 4(a) is a simulated noise free image from brain-web. Noise with standard deviation of 6.0% is added as shown in Fig. 4(b). The result of the denoising algorithm using the default parameters is shown in Fig. 4(c). The difference between the denoised image and the noise free image is shown in Fig. 4(d), whose power spectrum is shown in Fig. 4(e). It is obvious that the power spectrum is not white as expected. Entropy of the power spectrum image is 3.1955, MSE between the noise free image and the denoised image is 1.33×10^{-4} , and 1/SD value is 0.9149. These points are shown in Fig. 5(a) and Fig. 5(b), denoted by black cross. In a later section, we will show that these solutions are dominated solutions. Therefore, they are not the best possible solutions. Better parameters sets can be obtained through the proposed multiobjective optimization method.

4.3 Results of Proposed Algorithm

We ran the proposed optimization procedure using two different pairs of cost functions: MSE vs. Entropy and MSE vs. 1/SD. The Pareto fronts for both cases are shown in Fig. 5(a) and Fig. 5(b), respectively. Each of the Pareto fronts consists of 100 points that correspond to 100 non-dominated parameter sets. To check the optimized denoising results, 11 points on each Pareto fronts are chosen, and their corresponding values of cost functions are shown in Table 1(a) and Table 1(b), respectively. Each value of the cost functions in the table corresponds to one parameter set of the denoising algorithm.

4.4 Denoising Results Comparison

The 11 points on each Pareto front correspond to 11 parameter sets. Each parameter set from the Pareto front of MSE vs. Entropy is applied to the denoising algorithm, and two of the results are shown in Fig. 6(b) and Fig. 6(c). Results obtained by using parameter set of pareto front of $1/SD$ vs. MSE are shown in Fig. 6(e) and Fig. 6(f). Difference images are shown in Fig. 7(a), Fig. 7(b) and Fig. 7(c), while their corresponding power spectrums are shown in Fig. 7(d), Fig. 7(e), and Fig. 7(f), respectively. Comparing these results with those obtained by using the default parameters shown in Fig. 6(d), it is clear that results obtained by the filtering algorithm using the optimized parameters have more noise removed and preserve better structure information.. The Pareto front provides a set of good candidate solutions for denoising, which dominate the default parameter set provided by the authors.

4.5 Computational Time

The SPEA2 algorithm takes around 10 hours to complete the optimization procedure. In practice, this does not impose time constraint because the optimization is done off-line.

5. CONCLUSION

We have defined several cost functions to assess the quality of noise removal and structure information preservation for image filtering algorithms. These cost functions are minimized using SPEA2 algorithm by adjusting parameters associated with filtering algorithms. The proposed optimization procedure is applied to image denoising based on block matching and 3D collaborative filtering. Experimental results show that the proposed procedure greatly enhances the outcome of denoising methods. This method can be applied to many other denoising methods, and can be extended further by defining more cost functions and optimizing all the cost functions simultaneously.

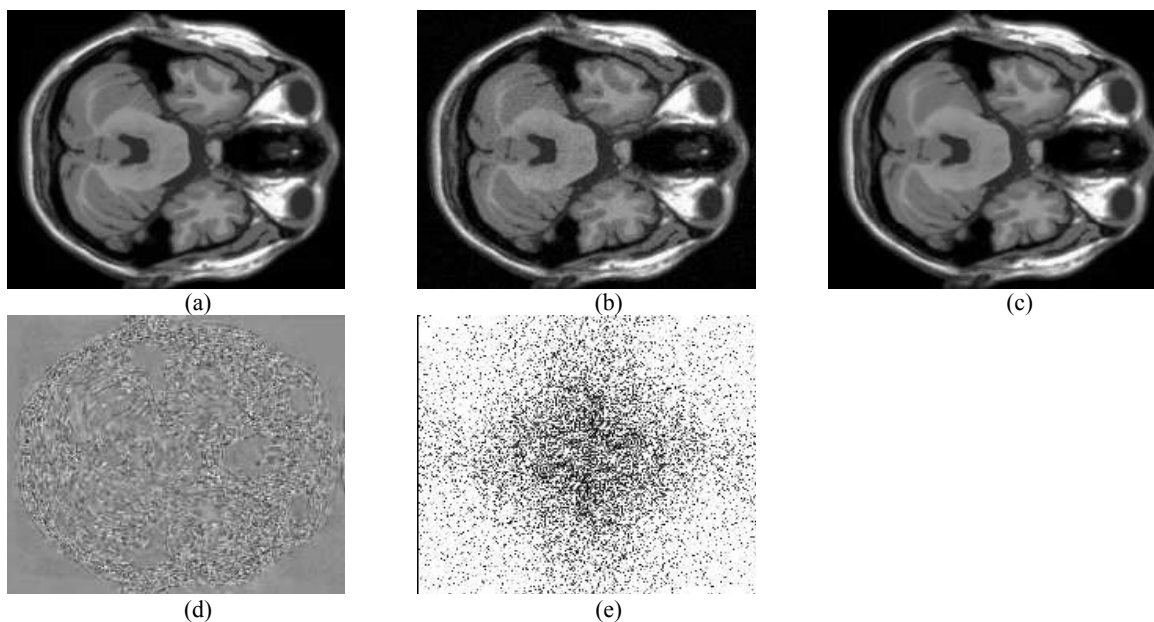


Fig. 4: (a) Noise free image, (b) Noised image, (c) Denoised image with default parameters, (d) Difference image between (a) and (c), (e) Power spectrum of (d)

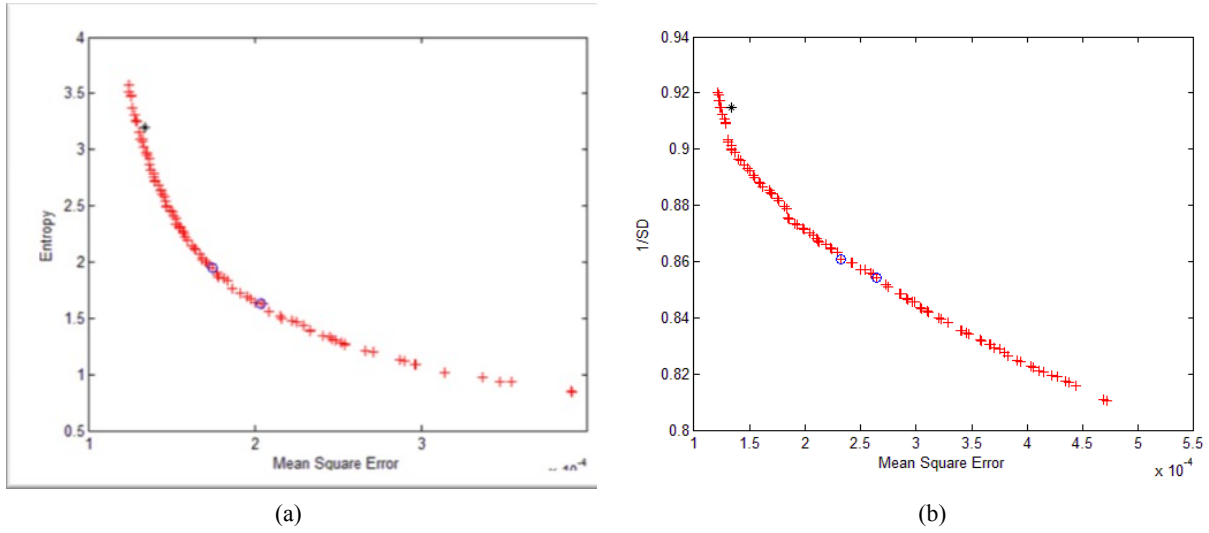


Fig. 5: (a) Pareto front for Entropy vs. MSE, (b) Pareto front for 1/SD vs. MSE

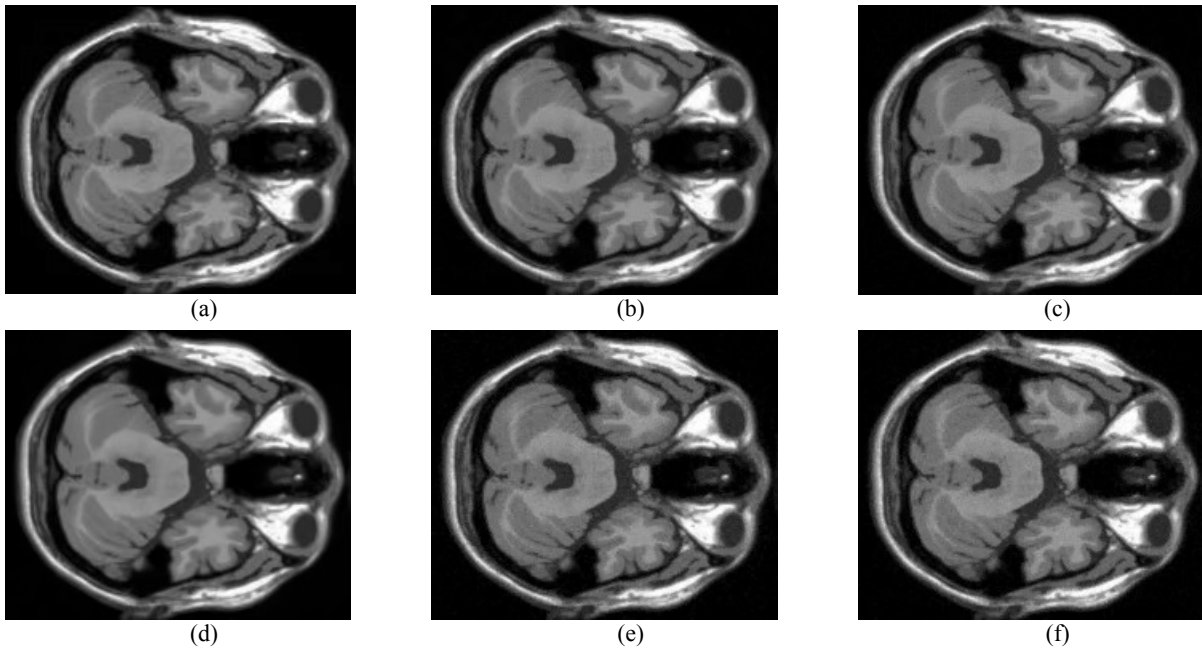


Figure 6: (a) Noise free image, (b) and (c) Denoised images obtained by using parameters from pareto front of Fig.5 (a), (d) Denoised image with default parameters, (e) and (f) Denoised images obtained by using parameters from pareto front of Fig.5 (b)

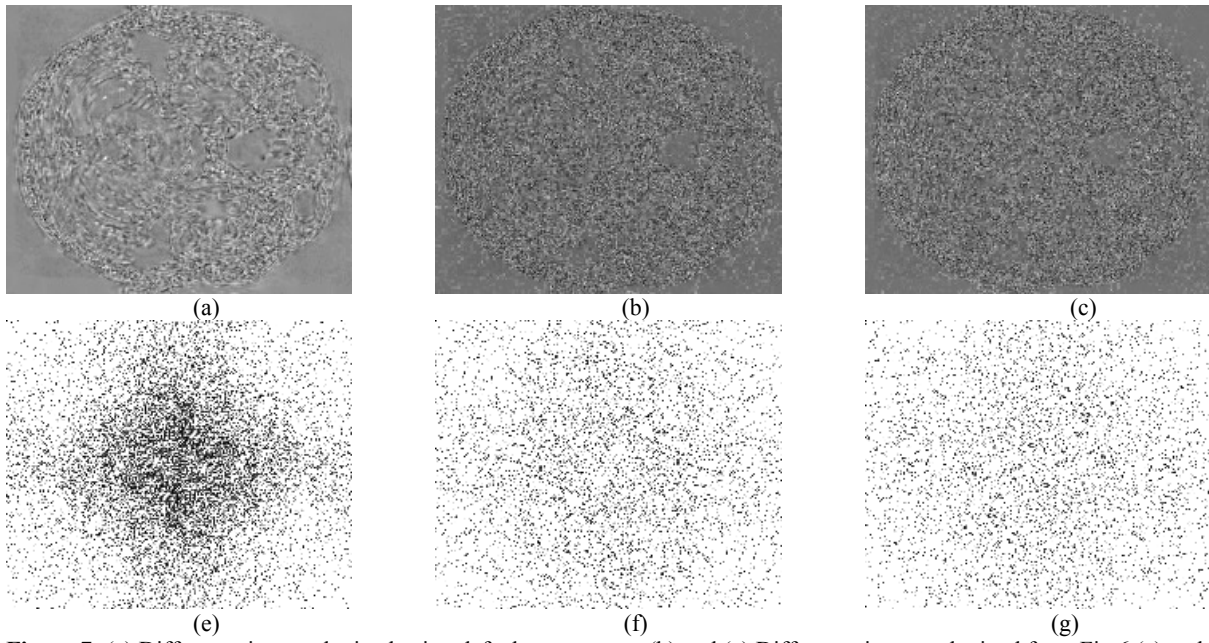


Figure 7: (a) Difference image obtained using default parameters, (b) and (c) Difference images obtained from Fig.6 (e) and Fig.6 (f), (e), (f) and (g) Corresponding power spectrums of (a), (b) and (c).

Table 1: (a) Values of cost functions Entropy vs. MSE, (b) Values of cost functions 1/SD vs. MSE

Parameter Set	Entropy of Power Spectrum	Mean Square error $\times 10^{-3}$	Parameter Set	1/SD	Mean Square error $\times 10^{-3}$
1	2.5844	0.1450	1	0.8825	0.1750
2	2.1943	0.1590	2	0.8645	0.2240
3	1.9527	0.1640	3	0.8610	0.2320
4	1.8323	0.1740	4	0.8544	0.2640
5	1.6268	0.1830	5	0.8465	0.2920
6	1.4774	0.2050	6	0.8395	0.3220
7	1.6268	0.2220	7	0.8345	0.3450
8	1.2644	0.2540	8	0.8247	0.3910
9	1.2020	0.2710	9	0.8225	0.4050
10	1.0176	0.3140	10	0.8174	0.4340
11	0.8474	0.3910	11	0.8103	0.4720

REFERENCES

- [1]. Zoroofi, R., A., Sato, Y., Tamura, S., Naito, H. "Mri artifact cancellation due to rigid motion in the imaging plane," IEEE Transactions on Medical Imaging, 15(6), 768-784, (1996).
- [2]. Lu, Q. Jiang, T. "Pixon-based image denoising with markov random fields," The Journal of Pattern Recognition Society, 34, (10), 2029-2039, (2001).
- [3]. Dabov, K., Foi, A., Egiazarian, K. "Image restoration by sparse 3d transform-domain collaborative filtering," Proc. SPIE Electronic Imaging, San Jose, California, 6812, 681 207-681 212 (2008).
- [4]. Jain, A., K., Murty, M. N., Flynn, P., J., "Data clustering: A review," ACM Computing Surveys, 31, 264-323 (1999).
- [5]. Collins, D., L., Zijdenbos, A., P., Kollokian, V., Sled, J., G., Kabani, N., J. Holmes, C., J., Evans, A., C. "Design and construction of a realistic digital brain phantom," IEEE Transactions on Medical Imaging, 17(3), 463-468, (1998).
- [6]. Veldhuizen, D., A., V., Lamont, G., B. "Multiobjective evolutionary algorithm test suites," Proc. ACM Symposium on Applied Computing, San Antonio, Texas, 351-57. (1999).
- [7]. Anastasio, M., A., Kupinski, M., A., Nishikawa, R., M. "Multiobjective genetic optimization of diagnostic classifiers with implications for generating receiver operating characteristic curves," IEEE Transactions on Medical Imaging, 18(8), 675-685, (1999).
- [8]. Anastasio, M., A. Kupinski, M., A., Nishikawa, R., M., "Optimization and froc analysis of rule based detection schemes using a multiobjective approach," IEEE Transactions on Medical Imaging, 17(6), 1089-1093, (1998).
- [9]. Li, J., Huang, A., Yao, J., Bitter, I., Summers, R., Pickhardt, P., Choi, J., "Automatic colonic polyp detection using multiobjective evolutionary technique," Proc. SPIE, California, USA, 1742-1750, (2006),
- [10]. Schaffer, J. D. "Multiobjective optimization with vector evaluated genetic algorithms," Genetic Algorithms and their Applications: Proc. First International Conference on Genetic Algorithms, Lawrence, Erlbaum, 93-100, (1985).
- [11]. Zitzler, E., Thiele, L., Laumanns, M., Fonseca, C., M., da Fonseca, V., G., "Performance assessment of multi-objective optimizers: An analysis and review," IEEE Transactions on Evolutionary Computation, 7, 117-132, (2003).
- [12]. Coello, C., A., C., "An updated survey of evolutionary optimization techniques: State of the art and future needs," Congress on Evolutionary Computation, Washington, D.C, 1, 3-13, (1999).
- [13]. Kostadin Dabov, Alessandro Foi, Vladimir Katkovnik and Karen Egiazarian, "Image denoising by sparse 3D transform-domain collaborative filtering", IEEE Transaction on Imaging Processing, vol. 16, no. 8, pp. 2080-2095 (2007).